Decoding, Performance Analysis, and Optimal Signal Designs for Coordinate Interleaved Orthogonal Designs

Dũng Ngọc Đào, *Member, IEEE,* and Chintha Tellambura, *Senior Member, IEEE*

***Abstract*— Space-time block codes (STBC) using coordinate interleaved orthogonal designs (CIOD) proposed recently by Khan and Rajan allow single-complex symbol decoding and offer higher data rates than orthogonal STBC. In this paper, we present the channel decoupling property of CIOD codes. A new general maximum likelihood method is derived, enabling the calculation of the symbol pair-wise error probability and union bound (UB) on symbol error rate (SER). Extensive simulation results show that the UB is within 0.1 dB from the simulated SER when SER < 10^{-2}. The UB thus can be used to accurately predict and optimize the performance of CIOD codes. Furthermore, a new signal design combining signal rotation and power allocation is presented for constellations with uneven powers of real and imaginary parts such as rectangular quadrature amplitude modulation.**

***Index Terms*— Space-time block codes, coordinate interleaved orthogonal designs, performance analysis.**

I. Introduction

ORTHOGONAL space-time block codes (OSTBC) [1], [2] are one of the most attractive space-time coding techniques to exploit the spatial diversity of the multiple-input multiple-output (MIMO) fading channels. The channel decoupling property of OSTBC implies that maximum likelihood (ML) detection of a vector of input symbols is equivalent to solving a set of scalar detection problems, one for each input symbol with minimal detection complexity. However, the code rate OSTBC is low when there are more than 2 transmit (Tx) antenna [1]–[3].

Recently, some alternative code designs have been introduced to improve the code rate of OSTBC, while the low decoding complexity is maintained. These codes are (1) STBC using coordinate interleaved orthogonal designs (CIOD) [4]–[6] and (2) minimum decoding complexity (MDC) quasi-orthogonal space-time block code (QSTBC) [7], [8]. The two codes are single (complex) symbol decodable. The maximal code rates of OSTBC, MDC-QSTBC, and CIOD codes are summarized in Table I for $2, \ldots, 8$ Tx antennas. Since CIOD codes offer equal or higher rates than the other codes, it is of interest to derive further properties of CIOD codes, which are unexplored in [4]–[6].

TABLE I
CODE RATES OF SINGLE-SYMBOL DECODABLE STBC

Codes	$M = 2$	$M = 3, 4$	$M = 5, 6$	$M = 7, 8$
OSTBC	1	3/4	2/3	5/8
MDC-QSTBC		1	3/4	3/4
CIOD		1	6/7	4/5

To achieve full diversity for CIOD codes, modulation symbols, such as quadrature amplitude modulation (QAM), need to be rotated an angle α [6]. The authors in [6] use the coding gain metric [9] to derive the optimal α for QAM. However, maximizing the coding gain is amount to minimizing the worst-case codeword pair-wise error probability (CPEP), which provides no guarantee for minimization of the symbol error rate (SER).

In this paper, we extent the methodology, which has been proposed in [10] to analyze the performance of MDC-QSTBC codes, and to provide new insights on CIOD codes. We first derive an equivalent channel representation for CIOD codes over MIMO channels. A new ML metric is also presented, enabling the derivation of symbol pair-wise error probability (SPEP). Hence the union bound on the symbol error rate (SER) can be easily evaluated. For all the tested cases, the union bound is within 0.1 dB of the simulated SER at medium and high signal-to-noise ratio (SNR). Therefore, this bound can be used to accurately analyze the performance of CIOD codes, and moreover, to optimize the signal rotation for arbitrary constellation. We furthermore present a new approach to design signal transformation for signals with unbalanced powers of real and imaginary parts such as rectangular QAM (QAM-R)[1]. The new method combines signal rotation and power (re)allocation yielding better performance than the existing ones in [6], [12] for QAM-R.

The rest of the paper is organized as follows. Section II briefly reviews the construction and properties of CIOD codes. The new equivalent channels and ML decoder of CIOD codes are introduced in Section III. The union bound on SER is presented in Section IV. Optimal signal rotations in terms of minimizing the union bound for various constellations are calculated. In Section V, the new signal transformation is proposed and optimized for QAM-R. Finally, conclusions are summarized in Section VI.

Manuscript received August 3, 2006; revised December 8, 2006; accepted January 22, 2007. The associate editor coordinating the review of this paper and approving it for publication is S. Zhou. This work is supported by The National Sciences and Engineering Research Council (NSERC) and Alberta Informatics Circle of Research Excellence (iCORE), Canada. This paper has been presented in part at the IEEE Military Communication Conference (Milcom), Washington D.C., USA, October 2006.

D. N. Đào was with the Department of Electrical and Computer Engineering, University of Alberta, Edmonton, Alberta T6G 2V4, Canada. He is now with the Department of Electrical and Computer Engineering, McGill University, Montreal, Québec, H3A 2A7, Canada (e-mail: dndung@ece.ualberta.ca).

C. Tellambura is with the Department of Electrical and Computer Engineering, University of Alberta, Edmonton, Alberta T6G 2V4, Canada (e-mail: chintha@ece.ualberta.ca).

Digital Object Identifier 10.1109/TWC.2008.060538.

[1]A rectangular QAM is constructed by two different m_1-ary and m_2-ary pulse amplitude modulation (m_1PAM and m_2PAM) [11].

II. Preliminaries

A. System Model

We consider data transmission over a uncorrelated MIMO channel with M-transmit (Tx) and N-receive (Rx) antennas. The channel gain h_{ik} $(i = 1, \cdots, M; k = 1, \cdots, N)$ between the (i,k)-th Tx-Rx antenna pair is assumed $\mathcal{CN}(0,1)$[2] and it is quasi-static frequency-flat fading channel [9], [13]. The receiver, but not the transmitter, completely knows the channel gains.

The space-time encoder parses data symbols into a $T \times M$ code matrix X of an STBC $\mathcal{X}$ as $X = \left[c_{ti}\right]_{\substack{t=1,\ldots,T \\ i=1,\ldots,M}}$, where c_{ti} is the symbol transmitted from antenna i at time t. The average energy of code matrices is constrained such that $\mathcal{E}_{\mathcal{X}} = \mathbb{E}[||X||_F^2] = T$, where $\mathbb{E}[\cdot]$ denotes average.

The received signals y_{tk} of the kth antenna at time t can be arranged in a matrix Y of size $T \times N$. Thus, one can represent the Tx-Rx signal relation as $Y = \sqrt{\rho} XH + Z$, where $H = [h_{ik}]_{\substack{i=1,\ldots,M \\ k=1,\ldots,N}}$, and $Z = [z_{tk}]_{\substack{t=1,\ldots,T \\ k=1,\ldots,N}}$, and z_{tk} are independently, identically distributed $\mathcal{CN}(0,1)$. The Tx power is scaled by ρ so that the average SNR at each Rx antenna is ρ, independent of the number of Tx antennas.

A block of K data symbols $(s_1, s_2, \cdots, s_K)$ can be mapped into a $T \times M$ space-time matrix as [1], [13]:

$$\mathcal{X} = \sum_{k=1}^{K} (a_k A_k + b_k B_k) \tag{1}$$

where A_k and B_k, $(k = 1, 2, \cdots, K)$ are $T \times M$ complex-valued constant matrices, a_k and b_k are the real and imaginary parts of the symbol s_k. We sometimes use the notation $\mathcal{X}_M(s_1, s_2, \ldots, s_K)$ to emphasize the transmitted symbols and the number of Tx antennas.

B. Construction of CIOD Codes

Since CIOD codes are constructed from OSTBC, for the readers' reference, we highlight several important properties of OSTBC [1], [2] that are essential for CIOD designs.

The dispersion matrices of an OSTBC $\mathcal{O}_M$ designed for M Tx antennas satisfy [14]:

$$A_i^\dagger A_i = B_i^\dagger B_i = \boldsymbol{I}_M, \qquad i = 1, 2, \cdots, K \tag{2a}$$
$$A_i^\dagger A_j + A_j^\dagger A_i = \mathbf{0}_M, \qquad 1 \le i \ne j \le K \tag{2b}$$
$$B_i^\dagger B_j + B_j^\dagger B_i = \mathbf{0}_M, \qquad 1 \le i \ne j \le K \tag{2c}$$
$$A_i^\dagger B_j + B_j^\dagger A_i = \mathbf{0}_M, \qquad 1 \le i, j \le K. \tag{2d}$$

We can use the set of parameters $\{M, T, K\}$ to describe an OSTBC [1]–[3].

The maximal code rate of existing OSTBC for $M = 2a-1$ or $M = 2a$, where a is any positive integer, is $\mathsf{R}_{\mathcal{O},M} = \frac{a+1}{2a}$ [2]. To guarantee the Tx power constraint, the space-time matrices of OSTBC are scaled by $\sqrt{\kappa}$. We can prove that

$$\kappa = \frac{1}{M\mathsf{R}_{\mathcal{O},M}}. \tag{3}$$

For example, the Alamouti code has $\kappa_2 = 1/2$. However, for notational brevity, κ is not always shown.

The CIOD code for M Tx antennas is constructed from two OSTBC components, $\mathcal{O}_{M_1}$ and $\mathcal{O}_{M_2}$, where $M = M_1 + M_2$, with parameter sets $\{M_1, T_1, K_1\}$ and $\{M_2, T_2, K_2\}$, respectively [6]. The matrices $\mathcal{O}_{M_1}$ and $\mathcal{O}_{M_2}$ are scaled by constants κ_1 and κ_2 to satisfy the power constraint.

Let $\bar{K}$ be the least common multiple (lcm) of K_1 and K_2, $n_1 = \bar{K}/K_1, n_2 = \bar{K}/K_2$, $\bar{T}_1 = n_1 T_1, \bar{T}_2 = n_2 T_2$. A block of $K = 2\bar{K}$ data (information) symbols $s_i = a_i + \mathrm{j}\, b_i$ ($\mathrm{j}^2 = -1), i = 1, 2, \ldots, K$ is mapped to the intermediate symbols x_k $(k = 1, 2, \ldots, K)$ as follows:

$$x_k = \begin{cases} a_k + \mathrm{j}\, b_{k+\bar{K}}, & k = 1, 2, \ldots, \bar{K}; \\ a_k + \mathrm{j}\, b_{k-\bar{K}}, & k = \bar{K}+1, \bar{K}+2, \ldots, K. \end{cases} \tag{4}$$

By this encoding rule, the coordinates of the symbols $s_1, s_2, \ldots, s_{\bar{K}}$ are interleaved with the coordinates of the symbols $s_{\bar{K}+1}, s_{\bar{K}+2}, \ldots, s_{2\bar{K}}$. Now we construct n_1 OSTBC code matrices $\mathcal{O}_{M_1,i}$ $(i = 1, 2, \ldots, n_1)$ and n_2 OSTBC code matrices $\mathcal{O}_{M_2,j}$ $(j = 1, 2, \ldots, n_2)$ and arrange them in the intermediate matrices $\mathcal{C}_1$ and $\mathcal{C}_2$ as

$$\mathcal{C}_1 = \begin{bmatrix} \mathcal{O}_{M_1,1}(x_1, x_2, \ldots, x_{K_1}) \\ \mathcal{O}_{M_1,2}(x_{K_1+1}, x_{K_1+2}, \ldots, x_{2K_1}) \\ \vdots \\ \mathcal{O}_{M_1,n_1}(x_{(n_1-1)K_1+1}, x_{(n_1-1)K_1+2}, \ldots, x_{\bar{K}}) \end{bmatrix},$$

$$\mathcal{C}_2 = \begin{bmatrix} \mathcal{O}_{M_2,1}(x_{\bar{K}+1}, x_{\bar{K}+2}, \ldots, x_{\bar{K}+K_2}) \\ \mathcal{O}_{M_2,2}(x_{\bar{K}+K_2+1}, x_{\bar{K}+K_2+2}, \ldots, x_{\bar{K}+2K_2}) \\ \vdots \\ \mathcal{O}_{M_2,n_2}(x_{\bar{K}+(n_2-1)K_2+1}, x_{\bar{K}+(n_2-1)K_2+2}, \ldots, x_{2\bar{K}}) \end{bmatrix}.$$

Hence, the size of $\mathcal{C}_1$ and $\mathcal{C}_2$ are $\bar{T}_1 \times M_1$ and $\bar{T}_2 \times M_2$, respectively. The CIOD code matrix is formulated by

$$\mathcal{C} = \begin{bmatrix} \sqrt{\kappa_1}\,\mathcal{C}_1 & \mathbf{0}_{\bar{T}_1 \times M_2} \\ \mathbf{0}_{\bar{T}_2 \times M_1} & \sqrt{\kappa_2}\,\mathcal{C}_2 \end{bmatrix}. \tag{5}$$

Thus the size of the CIOD code matrices are $T \times M$, where $T = \bar{T}_1 + \bar{T}_2 = n_1 T_1 + n_2 T_2$, $M = M_1 + M_2$.

The real and imaginary parts of symbols are separately transmitted over M_1 and M_2 antennas, respectively. Thus full diversity gain cannot be achieved. The solution is to rotate the real and imaginary parts of the input symbols and then to map the rotated symbols to CIOD code matrices. This ensures that the real and imaginary parts of the input symbols are spread over all Tx antennas. In the next section, we optimize the rotation angle based on a tight union bound on SER. As a preliminary step, we derive a new simplified Tx-Rx signal relation of CIOD codes, in which the equivalent channel can be shown explicitly.

III. Equivalent Channels and ML Decoder

Since the mapping rules of the real and imaginary parts of symbols s_k are known, one can write explicitly the dispersion matrices of these symbols. For notational convenience, we

[2]A mean-m and variance-σ^2 circularly complex Gaussian random variable is written by $\mathcal{CN}(m, \sigma^2)$. From now on, superscripts $^{\mathsf{T}}$, *, and † denote matrix transpose, conjugate, and transpose conjugate, respectively. An $n \times n$ identity and all-zero $m \times n$ matrices are denoted by $\boldsymbol{I}_n$ and $\mathbf{0}_{m\times n}$, respectively. The diagonal matrix with elements of vector $\boldsymbol{x}$ on the main diagonal is denoted by $\mathrm{diag}(\boldsymbol{x})$ and $\otimes$ denotes Kronecker product. $\Re(X)$ and $||X||_F$ represent the real part and Frobenius norm of matrix X, respectively.

reserve capital letters A and B for the dispersion matrices of OSTBC and use capital letters E and F for the dispersion matrices of CIOD codes. We also write $A_i(\mathcal{O}_{M_j})$ or $B_i(\mathcal{O}_{M_j})$ to denote the dispersion matrices of OSTBC $\mathcal{O}_{M_j}$ $(j = 1, 2)$.

There are $K = 2\bar{K}$ pairs of such matrices E_k, F_k $(i = 1, 2, \ldots, K)$; they can be explicitly written though they are quite lengthy. For example, the dispersion matrices of symbol s_1 are:

$$E_1 = \begin{bmatrix} A_1(\mathcal{O}_{M_1}) & \mathbf{0}_{T_1\times M_2} \\ \mathbf{0}_{(n_1-1)T_1\times M_1} & \mathbf{0}_{(n_1-1)T_1\times M_2} \\ \mathbf{0}_{T_2\times M_1} & \mathbf{0}_{T_2\times M_2} \\ \mathbf{0}_{(n_2-1)T_2\times M_1} & \mathbf{0}_{(n_2-1)T_2\times M_2} \end{bmatrix},$$

$$F_1 = \begin{bmatrix} \mathbf{0}_{T_1\times M_1} & \mathbf{0}_{T_1\times M_2} \\ \mathbf{0}_{(n_1-1)T_1\times M_1} & \mathbf{0}_{(n_1-1)T_1\times M_2} \\ \mathbf{0}_{T_2\times M_1} & B_1(\mathcal{O}_{M_2}) \\ \mathbf{0}_{(n_2-1)T_2\times M_1} & \mathbf{0}_{(n_2-1)T_2\times M_2} \end{bmatrix}.$$

We can write the CIOD codes using the dispersion form (1) as $\mathcal{C} = \sum_{k=1}^{K} (a_k E_k + b_k F_k)$.

To simplify our analysis, we first consider the number of Rx antennas is $N = 1$ and generalize for $N > 1$ later.

Let the channel vector be $\boldsymbol{h} = \begin{bmatrix} h_1 & h_2 & \ldots & h_M \end{bmatrix}^{\mathsf{T}}$, the Rx vector be $\boldsymbol{y} = \begin{bmatrix} y_1 & y_2 & \ldots & y_T \end{bmatrix}^{\mathsf{T}}$, the data vector $\boldsymbol{d} = \begin{bmatrix} a_1 & b_1 & a_2 & b_2 & \ldots & a_K & b_K \end{bmatrix}^{\mathsf{T}}$, the additive noise vector be $\boldsymbol{z} = \begin{bmatrix} z_1 & z_2 & \ldots & z_T \end{bmatrix}^{\mathsf{T}}$. Let C be a CIOD code matrix, the Tx-Rx signals becomes

$$\begin{aligned} \boldsymbol{y} &= \sqrt{\rho} C\boldsymbol{h} + \boldsymbol{z} = \sqrt{\rho} \sum_{k=1}^{K} (a_k E_k \boldsymbol{h} + b_k F_k \boldsymbol{h}) + \boldsymbol{z} \\ &= \sqrt{\rho} \begin{bmatrix} E_1\boldsymbol{h} & F_1\boldsymbol{h} & E_2\boldsymbol{h} & F_2\boldsymbol{h} & \ldots & E_K\boldsymbol{h} & F_K\boldsymbol{h} \end{bmatrix} \boldsymbol{d} + \boldsymbol{z}. \end{aligned} \tag{6}$$

In (6), the scalars κ_1 and κ_2 are not included for brevity. We can rewrite (6) equivalently as

$$\begin{bmatrix} \boldsymbol{y} \\ \boldsymbol{y}^* \end{bmatrix} = \sqrt{\rho} \begin{bmatrix} E_1\boldsymbol{h} & F_1\boldsymbol{h} & \ldots & E_K\boldsymbol{h} & F_K\boldsymbol{h} \\ E_1^*\boldsymbol{h}^* & F_1^*\boldsymbol{h}^* & \ldots & E_K^*\boldsymbol{h}^* & F_K^*\boldsymbol{h}^* \end{bmatrix} \boldsymbol{d} + \begin{bmatrix} \boldsymbol{z} \\ \boldsymbol{z}^* \end{bmatrix}. \tag{7}$$

Let $\bar{\mathcal{H}}_k = \begin{bmatrix} E_k\boldsymbol{h} & F_k\boldsymbol{h} \\ E_k^*\boldsymbol{h}^* & F_k^*\boldsymbol{h}^* \end{bmatrix}$ for $k = 1, 2, \ldots, K$, it follows

$$\bar{\mathcal{H}}_k^{\dagger}\bar{\mathcal{H}}_k = \operatorname{diag}\left(\hat{h}_1, \hat{h}_2\right) \triangleq \hat{\mathcal{H}}_1, \quad \text{for } 1 \le k \le \bar{K}, \tag{8a}$$

$$\bar{\mathcal{H}}_k^{\dagger}\bar{\mathcal{H}}_k = \operatorname{diag}\left(\hat{h}_2, \hat{h}_1\right) \triangleq \hat{\mathcal{H}}_2, \quad \text{for } \bar{K} < k \le K, \tag{8b}$$

$$\bar{\mathcal{H}}_k^{\dagger}\bar{\mathcal{H}}_l = \mathbf{0}_{2\times 2}, \quad \text{for } k \ne l. \tag{8c}$$

where $\hat{h}_1 = 2\sum_{i=1}^{M_1} |h_i|^2, \hat{h}_2 = 2\sum_{i=1}^{M_2} |h_i|^2$.

Thus if the two sides of (7) are multiplied by $\bar{\mathcal{H}}_k^{\dagger}$, one gets

$$\underbrace{\bar{\mathcal{H}}_k^{\dagger}\begin{bmatrix} \boldsymbol{y} \\ \boldsymbol{y}^* \end{bmatrix}}_{\bar{\boldsymbol{y}}_k} = \sqrt{\rho}\hat{\mathcal{H}}_p \underbrace{\begin{bmatrix} a_k \\ b_k \end{bmatrix}}_{d_k} + \underbrace{\bar{\mathcal{H}}_k^{\dagger}\begin{bmatrix} \boldsymbol{z} \\ \boldsymbol{z}^* \end{bmatrix}}_{\bar{\boldsymbol{z}}_k}. \tag{9}$$

where $p = 1$ if $1 \le k \le \bar{K}$ and $p = 2$ if $\bar{K} < k \le K$.

The matrix $\bar{\mathcal{H}}_k^{\dagger}$ plays the role of the spatial signature of the data vector d_k. Since the data vectors d_k can be completely decoupled, (9) can be used for ML detection. However, the noise vector $\bar{\boldsymbol{z}}_k$ is correlated with covariance matrix $\hat{\mathcal{H}}_p$, it needs to be whitened by a matrix $\hat{\mathcal{H}}_p^{-1/2}$ [15]. After this whitening step, (9) becomes

$$\hat{\mathcal{H}}_p^{-1/2}\bar{\boldsymbol{y}}_k = \sqrt{\rho}\hat{\mathcal{H}}_p^{1/2} d_k + \hat{\mathcal{H}}_p^{-1/2}\bar{\boldsymbol{z}}_k. \tag{10}$$

The matrices $\mathcal{H}_1 = \hat{\mathcal{H}}_1^{1/2}$ and $\mathcal{H}_2 = \hat{\mathcal{H}}_2^{1/2}$ can be considered the *equivalent channels* of CIOD codes.

The ML solution of (10) is

$$\hat{d}_k = \arg\min_{d_k} (\rho d_k^{\mathsf{T}}\hat{\mathcal{H}}_p d_k - 2\sqrt{\rho}\Re(\bar{\boldsymbol{y}}_k^{\mathsf{T}})d_k). \tag{11}$$

The result in (11) can be generalized for multiple Rx antennas. To this end, we include the scalars κ_1 and κ_2 for completeness. We can show that $\hat{h}_1 = 2\kappa_1 \sum_{j=1}^{N}\sum_{i=1}^{M_1} |h_{i,j}|^2$, $\hat{h}_2 = 2\kappa_2 \sum_{j=1}^{N}\sum_{i=1}^{M_2} |h_{i,j}|^2$, $\bar{\boldsymbol{y}}_k = \sum_{j=1}^{N} \bar{\mathcal{H}}_{k,n}^{\dagger} \begin{bmatrix} \boldsymbol{y}_n \\ \boldsymbol{y}_n^* \end{bmatrix}$, where $\boldsymbol{y}_n$ is the Rx vector of nth antenna, $\bar{\mathcal{H}}_{k,n} = \begin{bmatrix} E_k\boldsymbol{h}_n & F_k\boldsymbol{h}_n \\ E_k^*\boldsymbol{h}_n^* & F_k^*\boldsymbol{h}_n^* \end{bmatrix}$, $\boldsymbol{h}_n$ is the nth column of the channel matrix H.

From (9), the decoding of the real symbols a_k and b_k can be decoupled. However, since the symbols a_k and b_k are not transmitted over M channels, full diversity cannot be achievable. Hence, we need to spread out these symbols over M channels by applying a real unitary rotation R_p as

$$R_p = \begin{bmatrix} \cos(\alpha_p) & \sin(\alpha_p) \\ \sin(\alpha_p) & -\cos(\alpha_p) \end{bmatrix}, \quad (p = 1, 2),$$

to the data vectors d_k [6], [12]. Including the rotation matrix to (10) and (11), we have

$$\hat{\mathcal{H}}_p^{-1/2}\bar{\boldsymbol{y}}_k = \sqrt{\rho}\hat{\mathcal{H}}_p^{1/2} R_p d_k + \hat{\mathcal{H}}_p^{-1/2}\bar{\boldsymbol{z}}_k, \tag{12}$$

and

$$\hat{d}_k = \arg\min_{d_k} (\rho d_k^{\mathsf{T}} R_p^{\mathsf{T}}\hat{\mathcal{H}}_p R_p d_k - 2\sqrt{\rho}\Re(\bar{\boldsymbol{y}}_k^{\mathsf{T}})R_p d_k). \tag{13}$$

Some interesting facts can be drawn from the newly proposed decoder of CIOD codes. First, with OSTBC, the MIMO channel is decoupled into single-input single-output (SISO) channels and the equivalent channel gain is the Frobenius norm of the MIMO channel [16]. On the other hand, the MIMO channel becomes 2×2 diagonal channels with CIOD codes; the two entries of the diagonal are simply Frobenius norms of the first M_1 and the other M_2 columns of the MIMO channel matrix, where respectively, the real and imaginary parts of the rotated signal are transmitted on. Second, in contrast to the scalar detection of OSTBC, the detection of CIOD codes involves vector detection. Therefore, exact SER calculation becomes difficult. However, the calculation of symbol PEP is relatively simple as we will see in the next section.

IV. Union Bound on SER and Optimal Signal Designs

We first consider the data vectors $d_k = [a_k \;\; b_k]^{\mathsf{T}}$ for $1 \le k \le \bar{K}$. These data vectors are sent over the same equivalent channel $\hat{\mathcal{H}}_1^{1/2}$ and therefore they have the same error probability; we thus drop the subindex k for short. Let $d = [a\; b]^{\mathsf{T}}$ and $\hat{d} = [\hat{a}\; \hat{b}]^{\mathsf{T}}$ be the transmitted and the erroneous detected vectors, let $\delta_1 = a - \hat{a}$, $\delta_2 = b - \hat{b}$, $\Delta = [\delta_1\; \delta_2]^{\mathsf{T}}$. From

(12), the SPEP of the symbol pair d and $\hat{d}$ can be expressed by the Gaussian tail function as [17]

$$P(d \to \hat{d}|\hat{\mathcal{H}}_1) = Q\left(\sqrt{\frac{\rho|\hat{\mathcal{H}}_1 R_1 \Delta|^2}{4N_0}}\right) \tag{14}$$

where $N_0 = 1/2$ is the variance of the real part of the elements of the white noise vector $\hat{\mathcal{H}}_p^{-1/2}\bar{z}$ in (12). Let $\begin{bmatrix}\beta_1 & \beta_2\end{bmatrix}^{\mathsf{T}} = R_1\Delta$. We can apply the approach to derive the exact SPEP for MDC-QSTBC [10] to obtain the SPEP of CIOD codes as follows:

$$P_1(d \to \hat{d}) = \frac{1}{\pi}\int_0^{\pi/2}\left(1+\frac{\rho\kappa_1\beta_1^2}{4\sin^2\theta}\right)^{-M_1 N}\left(1+\frac{\rho\kappa_2\beta_2^2}{4\sin^2\theta}\right)^{-M_2 N} d\theta. \tag{15}$$

The above SPEP is given for symbols sent over the equivalent channel $\mathcal{H}_1$. For the symbols $s_k\,(\bar{K} < k \leq K)$ transmitted over the equivalent channel $\mathcal{H}_2$, the SPEP can be found similarly as

$$P_2(d \to \hat{d}) = \frac{1}{\pi}\int_0^{\pi/2}\left(1+\frac{\rho\kappa_2\bar{\beta}_1^2}{4\sin^2\theta}\right)^{-M_2 N}\left(1+\frac{\rho\kappa_1\bar{\beta}_2^2}{4\sin^2\theta}\right)^{-M_1 N} d\theta \tag{16}$$

where $\begin{bmatrix}\bar{\beta}_1 & \bar{\beta}_2\end{bmatrix}^{\mathsf{T}} = R_2\begin{bmatrix}\delta_1 & \delta_2\end{bmatrix}^{\mathsf{T}}$.

Assume that d_i, d_j, d_m, d_n, $(i, j, m, n = 1, 2, \ldots, L)$, are signals drawn from a constellation $\mathcal{S}$ of size L. From the SPEP expression (15) and (16), we can find the union bound on SER of CIOD codes with constellation $\mathcal{S}$ as

$$P_u(\mathcal{S}) = P_{u,1}(\mathcal{S}) + P_{u,2}(\mathcal{S}) \tag{17}$$

where $P_{u,1}(\mathcal{S}) = \frac{1}{L}\sum_{i=1}^{L-1}\sum_{j=i+1}^{L} P(d_i \to d_j)$ and $P_{u,2}(\mathcal{S}) = \frac{1}{L}\sum_{m=1}^{L-1}\sum_{n=i+1}^{L} P(d_m \to d_n)$.

For a fixed SNR, the union bound $P_u(\mathcal{S})$ depends on the constellation $\mathcal{S}$ and the rotation angles α_1 and α_2. Thus one can find the optimal values of α_1 and α_2 to minimize the union bound on SER.

Note that α_1 and α_2 can be optimized separately. We can run computer search to find the optimal values of α_1 and α_2. The run time for searching optimal values of α_1 and α_2 of a given constellation is only few minutes. However, we can further reduce the searching time by considering the following observation. In practice, $\mathcal{S}$ is usually symmetric via either horizontal or vertical axis of the Cartesian coordinate system. We can assume that $\mathcal{S}$ is symmetric via the vertical axis. If $\mathcal{S}$ is symmetric via the horizontal axis, we can always rotate the whole constellation an angle of $\pi/2$ to make it symmetric via the vertical axis.

Assume that $\alpha_2 = \pi/2 - \alpha_1$. Then, for each pair of symbols $(d_i, d_j) = \left([a_i,\ b_i]^{\mathsf{T}}, [a_j,\ b_j]^{\mathsf{T}}\right)$, we can find one and only one pair $(d_m, d_n) = \left([a_i,\ -b_i]^{\mathsf{T}}, [a_j,\ -b_j]^{\mathsf{T}}\right)$ so that $P_1(d_i \to d_j) = P_2(d_m \to d_n)$. Therefore, $P_{u,1}(\mathcal{S}) = P_{u,2}(\mathcal{S})$; and if α_{opt} is the optimal value of α_1, then $\pi/2 - \alpha_{opt}$ is optimal for α_2. Hence, we just write the value of α_1 and imply that the value of $\alpha_2 = \pi/2 - \alpha_1$.

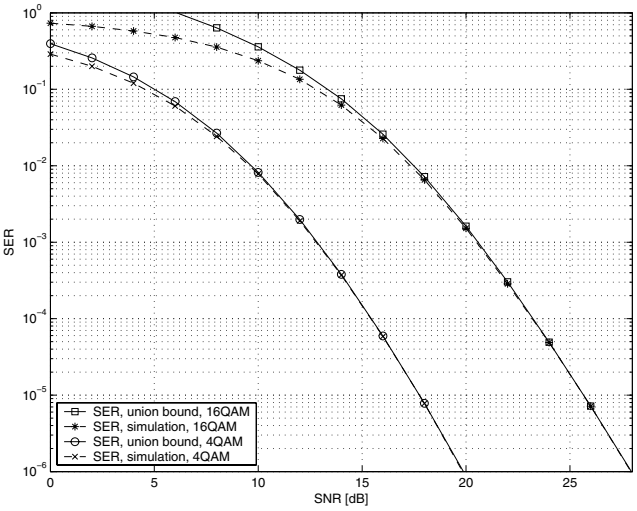

Fig. 1. Comparison of the union bound and simulated SER of a CIOD code with rate of 6/7 symbol pcu for 6 Tx antennas $(M_1 = 2, M_2 = 4)$, using 1 Rx antennas.

TABLE II
OPTIMAL ROTATION ANGLES OF POPULAR CONSTELLATIONS

Signal	(2, 1)[a]	(2, 2)	(2, 3)	(2, 4)	(3, 3)
4QAM	28.939°	30.417°	29.698°	29.003°	30.778°
4TRI	20.142°	13.883°	71.739°	68.687°	75.836°
8PSK	37.690°	39.216°	38.808°	38.534°	39.857°
8APSK	10.316°	11.528°	11.181°	11.000°	12.015°
8TRI	20.309°	45.000°	11.061°	9.430°	45.000°
8QAM-R	33.037°	31.834°	29.658°	28.626°	31.737°
8QAM-SR	12.234°	13.036°	12.925°	12.701°	13.173°
16PSK	3.485°	2.570°	2.832°	2.964°	2.200°
16TRI	19.236°	45.000°	47.116°	70.690°	45.000°
16QAM	31.436°	31.677°	31.557°	31.462°	31.704°

[a]The numbers in the parenthesis denote the values of M_1 and M_2.

The union bound on SER is plotted in Fig. 1 for a CIOD code for $M = 6$ Tx antennas $(M_1, M_2) = (2, 4)$. For the two examined constellations (4QAM, and 16QAM), and $\alpha_1 = 31.7175°$, the union bound becomes tight when SER $< 10^{-1}$ and even converges to the simulated SER at high SNR. Similar results can be found for different number of Tx antennas; details are omitted for brevity.

Numerical Examples

Since the union bound is very tight for SER < 10^{-2}, it can be used to optimize the values of rotation angles α_1 and α_1. The new optimal signal rotations for the popular constellations based on minimizing the SER union bound are summarized in Table II. Only the optimal values of α_1 are listed, the optimal values of $\alpha_2 = \pi/2 - \alpha_1$. The geometrical shapes of 8-ary constellations can be found in [10, Fig. 2]. Note that in Table II, the α_{opt} varies with the number of antennas M_1 and M_2.

It is of interest to examine which constellations have the best performance in term of SER; the tight SER union bound can be used for comparison. In Fig. 2, performances of different constellations are plotted for $(M_1, M_2) = (2, 4)$. Obviously, QAM signals yield the best performance compared

with other constellations of the same size. On the other hand, TRI constellations have the best minimum Euclidean distance; however, their performance is inferior to that of QAM signals. This observation is also confirmed for another combination of $(M_1, M_2) = (3, 3)$ in Fig. 3.

Our newly proposed rotation angles are only slightly different from the optimal rotation angles for QAM in terms of coding gain derived in [6]. Therefore the performance improvement is marginal, but note that [6] does not cover constellations other than QAM. Nevertheless, the SER upper bound is an useful tool to accurately analyze the performance of different constellations with signal rotations.

The unitary rotation has been used and optimized for various constellations. Nevertheless, non-unitary signal transformation can also be used and provides better performance for some signals as we will investigate in the next section.

V. Optimal Signal Rotation with Power Allocation

For QAM-R, e.g. 8QAM-R in [10, Fig. 2(a)], the average powers of the real and imaginary parts of the signal points are different. We may change the power allocation to the real and imaginary parts of QAM-R signals to get better overall SER.

To change the power allocation, the real and imaginary of QAM-R signals are multiplied by constants σ_1 and σ_2, respectively. For example, let $\mathcal{S}$ be a constellation with signal set $\mathcal{S} = \{d \mid d = a + \mathrm{j}\, b, a, b \in \mathbb{R}\}$, the new constellation with new power allocation is $\bar{\mathcal{S}} = \{\bar{d} \mid \bar{d} = \sigma_1 a + \mathrm{j}\, \sigma_2 b; a, b \in \mathbb{R}\}$. The average energy of the constellation $\bar{\mathcal{S}}$ is kept the same as that of $\mathcal{S}$, i.e. unitary. For example, the 8QAM-R with signal points $\{(\pm 3 \pm \mathrm{j}, \pm 1 \pm \mathrm{j})/\sqrt{48}\}$ has constraint equation for coefficients σ_1 and σ_2 as $5\sigma_1^2 + \sigma_2^2 = 6$. Hence, if the value of σ_1 is given, the value of σ_2 is known explicitly.

We still use (17) to calculate the union bound on SER of CIOD codes with signal rotation and power re-allocation; (15) can be rewritten to include the effects of power re-allocation as

$$\begin{bmatrix}\beta_1 \\ \beta_2\end{bmatrix} = \underbrace{\begin{bmatrix}\cos(\alpha_1) & \sin(\alpha_1) \\ \sin(\alpha_1) & -\cos(\alpha_1)\end{bmatrix}\begin{bmatrix}\sigma_1 & 0 \\ 0 & \sigma_2\end{bmatrix}}_{\bar{R}_1}\begin{bmatrix}\delta_1 \\ \delta_2\end{bmatrix}. \tag{18}$$

The total effect of signal rotation and power re-allocation is the non-unitary signal transform $\bar{R}_1$. Now the minimization of the union bound is based on two variables: σ_1 (or σ_2) and α_1. We run exhaustive computer search to find the optimal values of σ_1 and α_1. In fact, there is only single value of σ_1 so that the union bound is minimized; this value of σ_1 is the global solution of the union bound minimization. The optimal values of σ_1, σ_2 and α_1 are found as follows: $(\sigma_1, \sigma_2, \alpha_1) = (0.9055, 1.3784, 45.0^\circ)$ for 8QAM-R and $(\sigma_1, \sigma_2, \alpha_1) = (0.8972, 1.3487, 43.0^\circ)$ for 32QAM-R.

In Fig. 4, we compare the union bounds on SER of 8QAM-R and 32QAM-R using signal rotation of Khan-Rajan with $\alpha_1 = 31.7175^\circ$ [6], signal transformation of Wang-Wang-Xia [12, Theorem 6], and our new signal transformation for CIOD codes with $M = 4$ $(M_1 = 2, M_2 = 2), N = 1$. At SER = 10^{-6}, our new signal transformation yields 0.2 dB and 0.4 dB gains compared with the signal designs of Wang-Wang-Xia and Khan-Rajan, respectively. The BER of 8QAM-R also confirms the improvement of our newly proposed transformation over the existing ones.

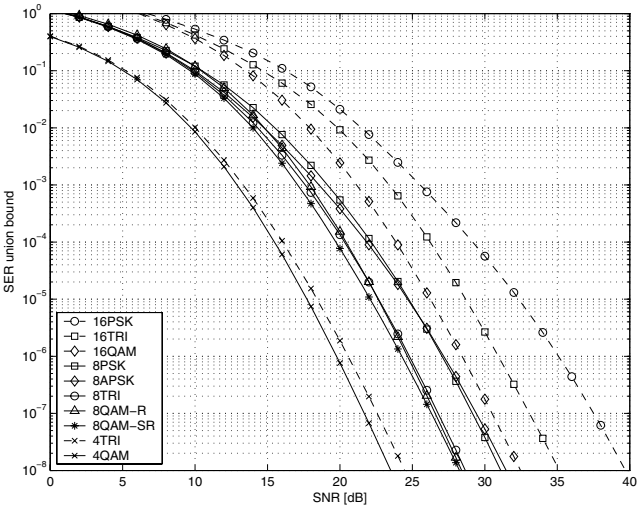

Fig. 2. SER union bound a CIOD code with rate of 6/7 symbol pcu for 6 Tx antennas $((M_1, M_2) = (2, 4))$, using 1 Rx antennas.

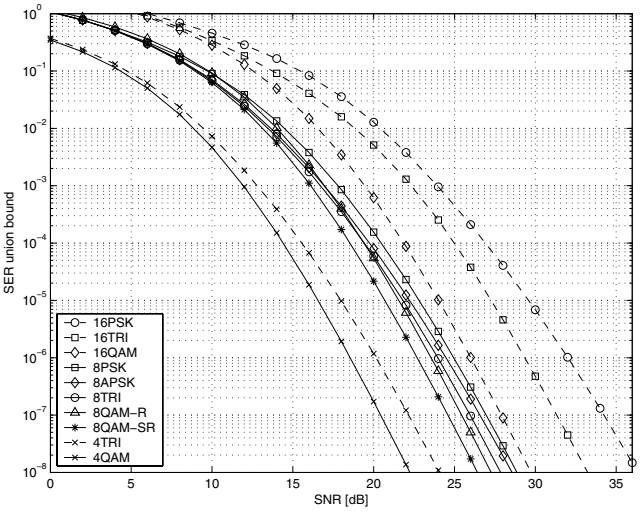

Fig. 3. SER union bound a CIOD code with rate of 3/4 symbol pcu for 6 Tx antennas $(M_1 = 3, M_2 = 3)$, using 1 Rx antennas.

The success of the new signal design comes from the fact that the powers of the real and imaginary parts of QAM-R are significantly different. We found that for other constellations with more balanced powers of the real and imaginary parts, new signal design even though can improve the performance, but insignificant.

VI. Conclusion

We have presented the equivalent channels for CIOD codes, enabling their decoding readily. The union bound on SER has been calculated, which is found to be within 0.1 dB of the simulated SER at medium and high SNR. Thus, it can be used to analyze the performance of CIOD codes and, more important, to optimize the signal rotation for any constellation with an arbitrary geometrical shape. Performances of CIOD

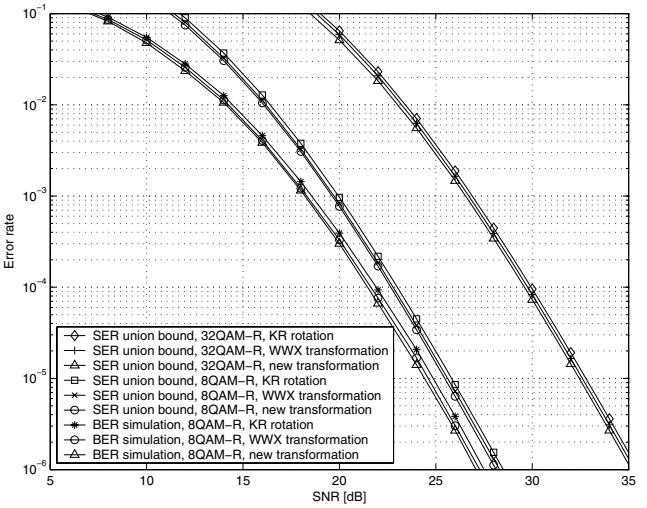

Fig. 4. BER and Union bound on SER of the rate-one CIOD code with rectangular 8QAM and 32QAM for 4 Tx antennas $(M_1 = 2, M_2 = 2)$, using 1 Rx antennas.

codes with different constellations such as QAM, PSK, TRI have been compared; among these signals, QAM yields the best performance. We further present a new approach to design signal transformation for signal with uneven powers of the real and imaginary parts such as QAM-R. The new signal designs for QAM-R outperform the existing ones. We have analyzed the performance of CIOD codes in uncorrelated Rayleigh channels. However, our results can be extended for correlated channels or other channel models with different distributions, such as Rician and Nakagami.

REFERENCES

[1] V. Tarokh, H. Jafarkhani, and A. R. Calderbank, "Space-time block codes from orthogonal designs," *IEEE Trans. Inform. Theory*, vol. 45, pp. 1456–1466, July 1999.

[2] X.-B. Liang, "Orthogonal designs with maximal rates," *IEEE Trans. Inform. Theory*, vol. 49, pp. 2468–2503, Oct. 2003.

[3] H. Wang and X.-G. Xia, "Upper bounds of rates of complex orthogonal space-time block codes," *IEEE Trans. Inform. Theory*, vol. 49, pp. 2788–2796, Oct. 2003.

[4] M. Z. A. Khan and B. S. Rajan, "Space-time block codes from co-ordinate interleaved orthogonal designs," in *Proc. IEEE Int. Symp. on Information Theory (ISIT)*, June 2002, p. 275.

[5] M. Z. A. Khan and B. S. Rajan, and M. H. Lee, "Rectangular co-ordinate interleaved orthogonal designs," in *Proc. IEEE GLOBECOM*, vol. 4, Dec. 2003, pp. 2004–2009.

[6] M. Z. A. Khan and B. S. Rajan, "Single-symbol maximum likelihood decodable linear STBCs," *IEEE Trans. Inform. Theory*, vol. 52, pp. 2062–2091, May 2006.

[7] C. Yuen, Y. L. Guan, and T. T. Tjhung, "Construction of quasi-orthogonal STBC with minimum decoding complexity from amicable orthogonal designs," in *Proc. IEEE Int. Symp. on Information Theory (ISIT)*, June 2004.

[8] ——, "Quasi-orthogonal STBC with minimum decoding complexity," *IEEE Trans. Wireless Commun.*, vol. 4, pp. 2089–2094, Sept. 2005.

[9] V. Tarokh, N. Seshadri, and A. R. Calderbank, "Space-time codes for high data rate wireless communication: Performance analysis and code construction," *IEEE Trans. Inform. Theory*, vol. 44, pp. 744–765, Mar. 1998.

[10] D. N. Đào and C. Tellambura, "Performance analysis and optimal signal designs for minimum decoding complexity ABBA codes," in *Proc. IEEE GLOBECOM*, Nov. 2006.

[11] N. C. Beaulieu, "A useful integral for wireless communication theory and its application to rectangular signaling constellation error rates," *IEEE Trans. Commun.*, vol. 54, pp. 802–805, May 2006.

[12] H. Wang, D. Wang, and X.-G. Xia, "On optimal quasi-orthogonal space-time block codes with minimum decoding complexity," *IEEE Trans. Inform. Theory*, submitted June 9, 2004. Its short version is published in *Proc. IEEE Int. Symp. on Information Theory* (ISIT), Sept. 2005.

[13] B. Hassibi and B. M. Hochwald, "High-rate codes that are linear in space and time," *IEEE Trans. Inform. Theory*, vol. 48, pp. 1804–1824, July 2002.

[14] G. Ganesan and P. Stoica, "Space-time block codes: a maximum SNR approach," *IEEE Trans. Inform. Theory*, vol. 47, pp. 1650–1656, Jan. 2001.

[15] C. Yuen, Y. L. Guan, and T. T. Tjhung, "Decoding of quasiorthogonal space-time block code with noise whitening," in *Proc. IEEE Personal, Indoor and Mobile Radio Communications Symp. (PIMRC)*, vol. 3, Sept. 2003, pp. 2166–2170.

[16] X. Li, T. Luo, G. Yue, and C. Yin, "A squaring method to simplify the decoding of orthogonal space-time block codes," *IEEE Trans. Commun.*, vol. 49, pp. 1700–1703, Oct. 2001.

[17] M. K. Simon and M.-S. Alouini, *Digital Communication over Fading Channels*, 1st ed. New York: Wiley, 2000.